THE JOURNAL OF PHYSICAL CHEMISTRY C

THE UNIVERSITY OF NEWCASTLE AUSTRALIA

Subscriber access provided by University of Newcastle, Australia

Article

Alcohol Oxidation at Platinum-Gas and Platinum-Liquid Interfaces: The Effect of Platinum Nanoparticle Size, Water Coadsorption and Alcohol Concentration

Hironori Tatsumi, Fudong Liu, Hui-Ling Han, Lindsay M. Carl, András Sápi, and Gabor A. Somorjai

J. Phys. Chem. C, **Just Accepted Manuscript** • DOI: 10.1021/acs.jpcc.7b01432 • Publication Date (Web): 22 Mar 2017

ACS Publications

The Journal of Physical Chemistry C is published by the American Chemical Society. 1155 Sixteenth Street N.W., Washington, DC 20036

Alcohol Oxidation at Platinum-Gas and Platinum-Liquid Interfaces: The Effect of Platinum Nanoparticle Size, Water Coadsorption and Alcohol Concentration

Hironori Tatsumi,[‡] *Fudong Liu,*[‡,§] *Hui-Ling Han,*[‡] *Lindsay M. Carl,*[†,‡] *Andras Sapi,*[‡,⊥] *and Gabor A. Somorjai**[,†,‡]

[†]Department of Chemistry, University of California, Berkeley, California 94720 and [‡]Lawrence Berkeley National Laboratory, Berkeley, California 94720, United States

ABSTRACT: Alcohol oxidation reaction over platinum nanoparticles with the size range from 2 to 8 nm deposited on mesoporous silica MCF-17 was studied in the gas and liquid phases. Among methanol, ethanol, 2- propanol and 2-butanol oxidations, the turnover frequency increased as the nanoparticle size became large in both reaction phases. The activation energy in the gas phase was higher than that in the liquid phase. Water coadsorption decreased the turnover rate of all the gas and liquid phase oxidations except for the gas phase 2-butanol case, while certain amount of water promoted 2-propanol oxidation the liquid phase. Sum frequency generation vibrational spectroscopy study and DFT calculation revealed that the alcohol molecules pack horizontally on the metal surface in low concentration and stand up in high

concentration, which affect the dissociation of β-hydrogen of the alcohol as the critical step in alcohol oxidation.

1. INTRODUCTION

The alcohol oxidation reaction is a crucial process for carbonyl compound production and energy conversion. Numerous studies have focused on improving catalyst performance, decreasing process cost, synthesizing new material, and further employing alcohols as new energy sources for fuel cells. Although there are a variety of ways to carry out the oxidation reactions, using transition metal catalyst with molecular oxygen is one of the promising ways to achieve both productivity and a low environmental impact. [1–9] Generally speaking, basic aldehyde and ketone products are manufactured in the gas phase oxidation at high temperature, while fine chemicals and pharmaceutical products are synthesized in the liquid phase at ambient temperature.[7] For example, methanol oxidation toward formaldehyde is carried out by gas-solid interfaces where silver and iron-molybdenum oxide catalysts are major players in the industrial scale[10–12], and also gold catalysts have attractive feature to lower reaction temperatures.[13] Furthermore, in order to improve the catalytic performance for selective oxidation of primary alcohols, bimetallic transition metal catalysts such as Au-Pd with suitable metal oxide supports have been studied in liquid-phase benzyl alcohol oxidation as a model reaction.[1,4] The reaction turnover rate and product selectivity are significantly affected by the reaction phase[16], however there are few studies which integrate the different effects on the reaction kinetics between gas and liquid phase under similar conditions. Therefore, we have studied these properties by using size controlled platinum nanoparticles (Pt NPs) and sum frequency generation (SFG) vibrational spectroscopy techniques.[17–21] Here we report our investigation of methanol, ethanol, 2-propanol

and 2-butanol oxidation reactions and compare the results to give a general knowledge on how each alcohol molecule behaves on the catalyst surface in various conditions.

2. EXPERIMENTAL SECTION

2.1. Size Control of Platinum Nanoparticles Loaded in MCF-17

Platinum nanoparticles (Pt NPs) were synthesized by PVP-assisted polyol process in ethylene glycol.[17–19,21] The average sizes for the nanoparticles were 2, 4, 6 and 8 nm respectively with the narrow size distributions as determined by transmission electron microscopic (TEM) images (See Supporting Information for details). In order to study the catalytic alcohol oxidation reaction with molecular oxygen in the gas and liquid phases, we chose the mesoporous silica MCF-17 as the Pt support.[22,23] MCF-17 has wide pore size ranges from 15 to 50 nm which are adequate to incorporate the sub 10 nm Pt NPs. The amount of Pt loaded into the support was measured by inductively coupled plasma atomic emission spectroscopy (ICP-AES). The mass loadings of Pt in each catalyst were from 0.4 to 0.7 wt. %.

2.2. Thin Film Platinum Catalyst for Sum Frequency Generation Vibrational Spectroscopy

The thin film samples for sum frequency generation (SFG) vibrational spectroscopy of 2-propanol oxidation were prepared by depositing Langmuir-Blodgett films[24,25] of silica embedded 4 nm Pt NPs on sapphire prisms followed by calcination in air at 550°C for 3 h. To prepare 4 nm Pt NPs embedded in silica, Pt nanoparticle ethanol suspension and tetraethyl orthosilicate were mixed with ethanol, to which ammonium hydroxide was added dropwise within 5 min under stirring. The mixture was then sonicated for 2 h. The product was precipitated by hexane and collected by centrifugation.[19]

2.3. Catalytic Oxidation Study

Various alcohol oxidation reactions were investigated in the gas and liquid phases using Pt NPs loaded into MCF-17 with pure anhydrous alcohol; methanol, ethanol, 2-propanol and 2-butanol from Aldrich. For gas phase catalysis, the reactor was typically filled with 10 Torr of alcohol, 50 Torr of oxygen and 710 Torr of helium. The reaction temperature was at 60°C in methanol, ethanol and 2-propanol oxidations, and 80°C in 2-butanol oxidation. The products were detected by a gas chromatography (GC) with a thermal conductivity detector.

For liquid phase catalysis, the reactions were carried out in a 100 ml stirred Parr reactor covered by heating tape. The reactor was typically filled with 10–30 mg of Pt/MCF-17 catalyst dispersed in 15 ml of liquid alcohol. The mixture was sealed, purged by pure oxygen, and then sealed at 1 bar oxygen atmosphere. Magnetic stirring was set at a certain speed and the mixture was kept at 60 °C. For 2-butanol oxidation reaction, typical oxygen pressure was 3 bar, and the reaction temperature was 80°C. After 1–3 h of reaction, the reactor was cooled to 45 °C. The gas in the reactor was transferred into the evacuated gas phase reactor connected to the GC to analyze the reactants and products in the gas phase. The liquid in the reactor was centrifuged to remove the solid catalyst. The supernatant was then injected into the GC to analyze the reactants and products in the liquid phase.

For the gas-phase reactions, catalytic activity and product selectivity were typically characterized at alcohol conversions below 30 %, whereas for the liquid-phase reactions, they were typically characterized at oxygen conversions between 20–40 % (corresponding to alcohol conversions of 1–4 %). Catalytic activity of the platinum catalysts was described in terms of turnover frequency (TOF) normalized to the number of active sites. The number of active sites

for each catalyst was calculated based on platinum particle size and mass loading characterized by TEM and ICP-AES, respectively. In addition, ethylene hydrogenation method was used to measure the actual number of active sites of the platinum catalysts and to confirm that calculation of turnover frequency (TOF) based on particle size is appropriate approach to study particle size effect on catalytic activity. The hydrogenation reaction was carried out in a gold-coated batch-reactor equipped with a boron nitride substrate heater and a circulation pump for gas mixing. The reactor was filled with 10 Torr of ethylene, 100 Torr of hydrogen and 660 Torr of helium at 25°C. Each catalyst was dispersed in ethanol and drop-casted on SiO_2 chips, and then set on a boron nitride substrate heater.

The products of the methanol oxidation reaction were carbon dioxide (CO_2), formaldehyde and methyl formate as a coupling product. The products of the other alcohol oxidation reactions were CO_2 and corresponded carbonyl compounds; acetaldehyde (Ethanol), acetone (2-Propanol) and 2-butanone (2-Butanol). No acid and ester products were detected in our experiments.

2.4. Sum Frequency Generation Vibrational Spectroscopy

Sum frequency generation (SFG) vibrational spectroscopy is using secondary nonlinear optical effect, which is highly selective toward the interfaces. This is one of the effective techniques to obtain the molecular orientations on the catalyst surface under reaction conditions. In our experiments, the infrared frequency was scanned from 2800 to 3600 cm^{-1} and its energy was ~100 μJ. The nonresonant frequency used was 532 nm (40 μJ). Sum frequency light was detected by a photomultiplier connected with a gated integrator. The polarization combination used in the experiment was ppp, which refers to perpendicular polarization for all beams relative to the sample surface. The data points in the spectra shown in this paper typically are comprised

of an average of 400−1000 individual measurements. In the 2-propanol SFG analysis, the reaction phase effect was examined under reaction condition. For the gas phase analysis, the sample was placed in the cell, then pure oxygen was bubbled through 2-propanol and sent through the cell at 18°C. For the liquid phase analysis, liquid 2-propanol was passed through the cell using a peristatic pump.

3. RESULTS AND DISCUSSION

3.1. Reaction Rate Comparison of Catalytic Alcohol Oxidation Reactions in the Gas and Liquid Phases

Catalytic activity of platinum catalysts for alcohol oxidation reactions, namely methanol, ethanol, 2-propanol, and 2-butanol oxidation, was summarized to reveal the effect of carbon number and reaction medium on total turnover rate and activation energy (Ea). The TOF values were calculated by normalizing the total conversion rate to the number of active sites. The number of active sites was calculated based on platinum nanoparticle size measured by TEM. However, it is noteworthy to mention that the TOF values calculated in this way might underestimate the effect of PVP capping agents and variations in the distribution of nanoparticle size. Accordingly, ethylene hydrogenation method was used to measure the actual number of active sites. Ethylene hydrogenation is widely used to quantify the number of active sites of platinum catalysts as the reaction is insensitive to platinum particles size and shape. The actual number of active sites measured by ethylene hydrogenation was indeed smaller than the number of active sites calculated exclusively based on particle size, which led to slightly higher TOF values. Nevertheless, the change in TOF as a function of particles size was comparable for both

methods. As a consequence, TOF values calculated based on particle size is unlikely to impose a bias on the size effect.

Figure 1 compares total TOFs for oxidation reactions on 6 nm Pt NPs loaded in MCF-17 in the gas and liquid phases. In the gas phase reaction, methanol oxidation result shows the highest TOF value; 10 molecules·site^{-1}·s^{-1} among C1-C4 alcohol oxidation reactions, whereas the other TOFs were 3.2 (Ethanol), 1.2 (2-Propanol) and 11.4 molecules·site^{-1}·s^{-1} (2-Butanol: 80°C) respectively. In the liquid phase, the TOF values of alcohol oxidation reaction were 0.9 (Methanol), 2.1 (Ethanol), 0.2 (2-Propanol) and 3.1 molecules·site^{-1}· s^{-1} (2-Butanol: 3 bar O_2, 80°C) respectively. In the methanol oxidation in the gas phase, the formate intermediate seems to be highly active compared with the other intermediate species in the other alcohol oxidations, which may lead to the large TOF.

The molecular amount ratios of alcohol to oxygen were 1 to 5 in the gas phase (0.8 mmol of alcohol vs 4.1 mmol of O_2), however those ratios in the liquid phase were higher than those in the gas phase due to the much higher alcohol density (Methanol Ox.: 591 mmol of methanol vs 0.2 mmol O_2, Ethanol Ox.: 413 mmol of ethanol vs 0.2 mmol O_2, 2-Propanol Ox.: 320 mmol of 2-propanol vs 0.2 mmol O_2, 2-Butanol Ox.: 250 mmol of 2-butanol vs 0.6 mmol of O_2). In order to mitigate the contrast, the alcohol was diluted with heptane to 1:1000 ratios in the liquid phase; Alcohol vs O_2 ratios were 1:0.9 (Methanol), 1:1.3 (Ethanol) and 1:1.7 (2-Propanol). Heptane is used as a neutral solvent which has small effect on reaction rate, size dependence, and activation energy in these reactions.[18,19] The TOFs in the liquid phase after heptane dilution were 0.001 (Methanol), 0.04 (Ethanol) and 0.004 molecules·site^{-1}·s^{-1} (2-Propanol) respectively, which exhibits 80~10000 times lower activity compared to the gas phase reaction under comparable concentration conditions. Although the reactant contents ratios are not exactly same between in

the gas and liquid phase (diluted), these results suggests that the alcohol molecular density has great impact on the alcohol oxidation reaction kinetics.

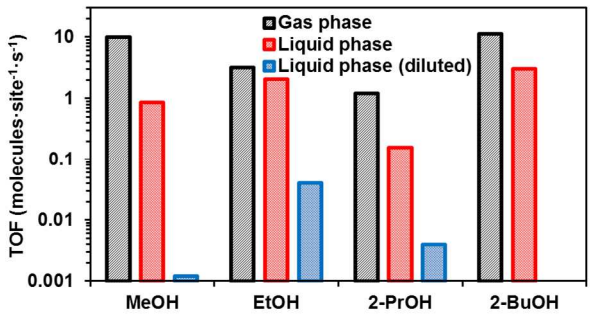

Figure 1. The total TOFs of alcohol oxidations over 6 nm Pt/MCF-17. Gas phase: 10 Torr alcohol, 50 Torr O_2, 60 °C (C1-C3 alcohol) and 80°C (2-butanol). Liquid phase: 15 ml alcohol, dissolved oxygen under 1 bar (C1-C3 alcohol) and 3 bar (2-butanol), 60 °C (C1-C3 alcohol) and 80°C (2-butanol). Liquid phase (diluted): 15ml heptane, 15µl alcohol with dissolved oxygen under 1 bar, 60 °C.

3.2. Activation Energy Comparison of Catalytic Alcohol Oxidation Reactions in the Gas and Liquid Phases

The activation energies of alcohol oxidation reactions over 4nm Pt/MCF-17 catalyst were summarized in Figure 2. In the gas phase, the activation energies were found to be 190 (Methanol), 200 (Ethanol), 147 (2-Propanol) and 119 kJ/mol (2-Butanol) respectively. Interestingly, these values became 2~6 times lower in the liquid phase; 30 (Methanol), 39 (Ethanol), 62 (2-Propanol) and 64 kJ/mol (2-Butanol) respectively. These different activation energies correlated with the reaction phase may due to the following reasons; the different mass transfer conditions of oxygen and different alcohol molecule orientation on the surface. As the catalyst is covered by solvent; alcohol and/or heptane in the liquid phase, the oxygen has

difficulty in attaching to the reaction active site. Besides the oxygen diffusion coefficient (D_{O2}) in the liquid phase is much smaller than that in the gas phase. (e.g. $D_{O2\ in\ water,\ 283K}$: 1.54×10^{-5} cm^2/s, $D_{O2\ in\ N2,\ 1\ atm,\ 273K}$: 0.181 cm^2/s)[26,27] The oxygen mass transfer through the liquid layer surrounding the Pt NPs is critical for alcohol oxidation in the liquid phase and also results in a lowering of the activation energy.[28,29] Furthermore different reaction mechanisms in the gas−solid and liquid−solid interface, which is discussed in SFG Analysis and DFT calculation sections, may affect the activation energy.

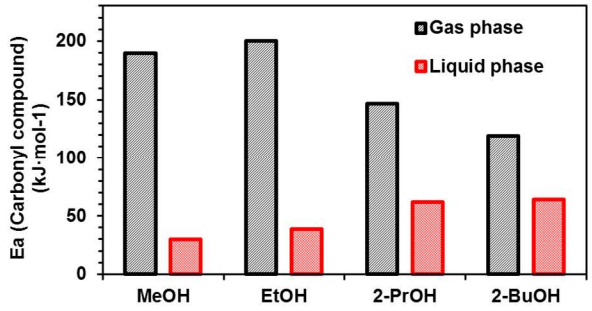

Figure 2. Activation energies of carbonyl compounds; formaldehyde (Methanol), acetaldehyde (Ethanol), acetone (2-Propanol) and 2-butanone (2-Butanol) in the gas and liquid phase alcohol oxidations over 4 nm Pt/MCF-17.

3.3. Influence of Platinum Nanoparticle Size on Reaction Rate and Product Selectivity

In this section, we summarized the Pt NPs size dependence on the TOF and product selectivity of catalytic alcohol oxidation reactions.

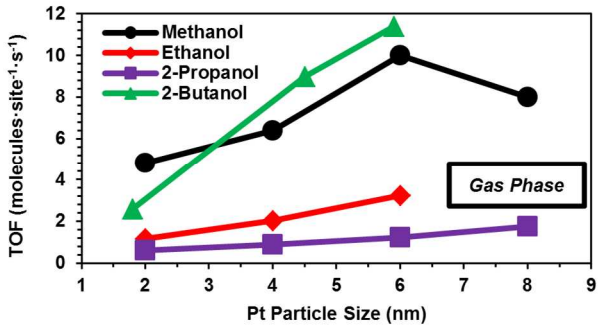

Figure 3. Size dependence of total TOFs in the gas phase: 10 Torr alcohol, 50 Torr O_2, 60 °C (C1-C3 alcohol) and 80°C (2-butanol).

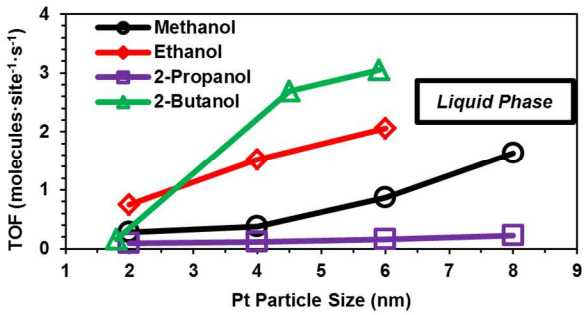

Figure 4. Size dependence of total TOFs in the liquid phase: 15 ml alcohol, dissolved oxygen under 1 bar (C1-C3 alcohol) and 3 bar (2-butanol), 60 °C (C1-C3 alcohol) and 80°C (2-butanol).

In the gas phase, the TOFs became 2~6 times larger as the particle size increases in all alcohol oxidation reactions. In the liquid phase, the TOFs showed same tendency in all alcohol oxidation reactions, which increased 2~19 times with the particle size grew. (Figure 3 and Figure 4, See Supporting Information in detail)

A similar characteristic of increasing specific activity with the Pt particle sizes has been reported in electrocatalytic methanol oxidation and oxygen reduction reaction.[30–33] Smaller Pt NPs have larger fractions of corner and edge atoms on their surface, which can bind certain

oxygenated species more strongly than alcohol species. Dehydrogenation of alcohol adsorbate on the Pt surface by oxygenated species is believed as the rate-determining step,[34,35] hence excessive amount of oxygenated species block the surface to interrupt the reaction kinetics.

The selectivity toward carbonyl compound products was summarized in Figure 5 and 6. In the gas phase, the selectivity showed 21-37% for formaldehyde (Methanol), 97% for acetaldehyde (Ethanol), 100% for acetone (2-propanol) and 94-98% for 2-butanone (2-butanol: 80°C) in the 2-8 nm range alcohol oxidation reactions. In the liquid phase, it showed 74-84% for formaldehyde (Methanol), 98% for acetaldehyde (Ethanol), 100% for acetone (2-propanol) and 93-99% for 2-butanone (2-butanol: 80°C) in these range. As a result, the Pt particle size didn't affect the reaction selectivity. Most of the alcohols were converted towards corresponding carbonyl compounds. Interestingly, the product selectivity of methanol oxidation is obviously different between gas and liquid phase. The significantly lower selectivity of methanol oxidation in the gas phase may due to the high activity of formaldehyde which can easily convert to methyl formate and CO_2 in the presence of surface oxygen .[17,36,37] On the other hand, the lack of surface oxygen due to the slower diffusion rate in the liquid phase, may limit the sequential H abstraction and O addition from formaldehyde to formate (HCOO) species which can convert to the byproducts.

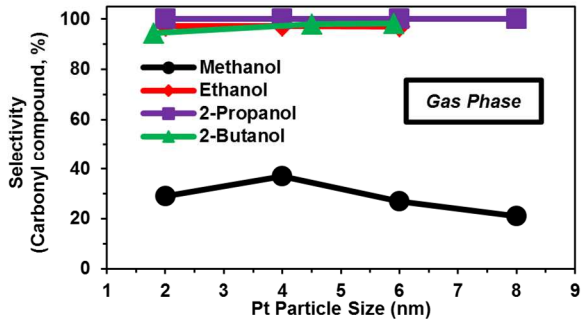

Figure 5. Size dependence of product selectivity in the gas phase: 10 Torr alcohol, 50 Torr O_2, 60 °C (C1-C3 alcohol) and 80°C (2-butanol). Carbonyl compound: formaldehyde (Methanol), acetaldehyde (Ethanol), acetone (2-Propanol) and 2-butanone (2-Butanol).

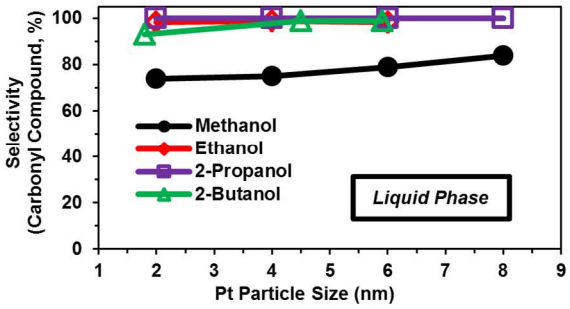

Figure 6. Size dependence of product selectivity in the liquid phase: 15 ml alcohol, dissolved oxygen under 1 bar (C1-C3 alcohol) and 3 bar (2-butanol), 60°C (C1-C3 alcohol) and 80°C (2-butanol).

3.4. Water Coadsorption Effect on Reaction Rate and Product Selectivity

Water is one of the products of alcohol oxidation reactions; its coadsorption on the catalyst active site may influence on the reaction turnover rate and product selectivity. Therefore we studied the water coadsorption effect on the alcohol oxidation reaction in the gas and liquid phases, which revealed unique characteristics. For the gas phase oxidations, the reactor was typically filled with 1−10 Torr water vapor, 10 Torr of alcohol, 50 Torr of oxygen and helium as balanced at 770 Torr, and 4 nm Pt NPs loaded in MCF-17 was used at 60°C. In 2-butanol oxidation, the 6 nm Pt NPs was used at 80°C. For the liquid phase oxidation, the reactor was typically filled with 7.5-15 ml pure alcohol, 0-7.5 ml distilled water (totally 15 ml volume),

dissolved oxygen under 1 bar, and 4 nm catalyst was used at 60 °C. In 2-butanol oxidation, 6 nm catalyst and 3 bar oxygen was used at 80°C. All data was normalized by the TOF value without water (X = 0).

Dramatic loss of catalytic activity was observed in C1-C3 alcohol oxidation reactions. Especially 1 Torr of added water vapor ($X_{water\ ratio}$= 0.1) resulted in as low as 36 (Methanol) and 27% (2-Propanol) of the water-free reaction activity (Figure 7). In C1-C3 alcohol oxidation reaction, the relative TOFs decreased to 0 when the water ratio is equal to each alcohol quantity, which means catalyst active sites were fully covered by the water. When it comes to the 2-butanol oxidation, different tendency was shown using 6 nm Pt NPs loaded in MCF-17. The water did not poison the reaction, the relative TOF still remained 84% of the water-free reaction activity at $X_{water\ ratio}$= 1. In the liquid phase alcohol oxidation reaction, water coadsorption effect on the TOF showed different tendency in each case (Figure 8). In the methanol and ethanol oxidation reactions, the relative TOFs were gradually decreased to 0 when the water ratio was equal to each alcohol quantity. In the 2-propanol oxidation reaction, the relative TOFs were increased 4 times higher compared to pure liquid alcohol by added water ($X_{water\ ratio}$= 0.8). Further increment in the water concentration resulted in the decline of activity. In the 2-butanol oxidation reaction, only 1 ml water affected the relative TOF decrease to 12% of the water-free reaction activity.

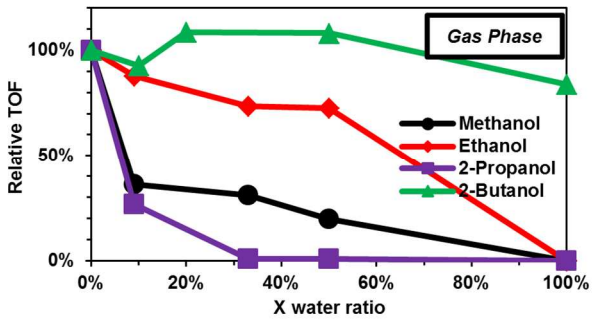

Figure 7. Water coadsorption effect on TOF of alcohol oxidations in the gas phase: 10 Torr alcohol, 1-10 Torr water vapor, 50 Torr O_2, 4 nm catalyst at 60°C (C1-C3 alcohol) and 6 nm catalyst at 80°C(2-butanol). All data was normalized by the TOF value without water (X = 0).

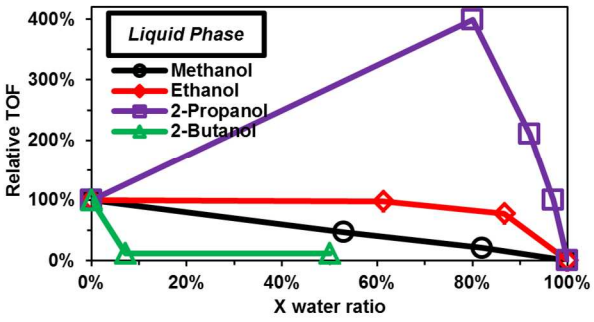

Figure 8. Water coadsorption effect on TOF of alcohol oxidations in the liquid phase: 7.5-15 ml pure alcohol, 0-7.5 ml distilled water, in total 15 ml volume, dissolved oxygen under 1 (C1-C3 alcohol) and 3 bar (2-butanol), 4 nm catalyst at 60 °C (C1-C3 alcohol) and 6 nm catalyst at 80°C(2-butanol). All data was normalized by the TOF value without water (X = 0).

The hydrophilicity of alcohol seems to be correlated with these phenomena. Methanol, ethanol and 2-propanol are miscible in water, while 2-butanol can be soluble by 12.5 g in 100 ml water due to the hydrophobic alkyl chain.[38] Pt NPs are covered by PVP capping agent which has amphiphilicity. In the gas phase where alcohol and water vapor can move freely, C1-C3 alcohol allows water to cover the Pt active site leading to poison the reaction progress. On the other hand, once 2-butanol attaches to the metal surface, it does not allow water to coadsorb on the catalyst. In the liquid phase where high concentrated alcohol exists around the catalyst, specific amount of water prompted the reaction turnover in 2-propanol oxidations. Meanwhile, water preferably gather around the catalyst due to the hydrophobicity of 2-butanol, poison the 2-butanol oxidation significantly in the liquid phase.

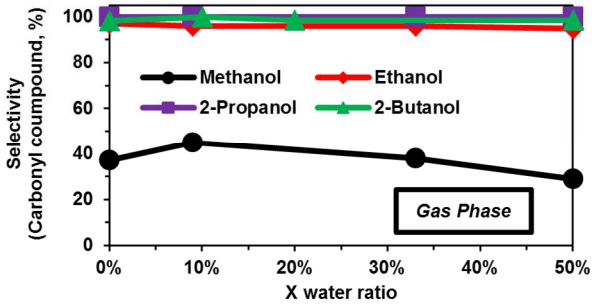

Figure 9. Water coadsorption effect on product selectivity of alcohol oxidations in the gas phase: 10 Torr alcohol, 1-10 Torr water vapor, 50 Torr O_2, 4 nm catalyst at 60 °C (C1-C3 alcohol) and 6 nm catalyst at 80 °C(2-butanol).

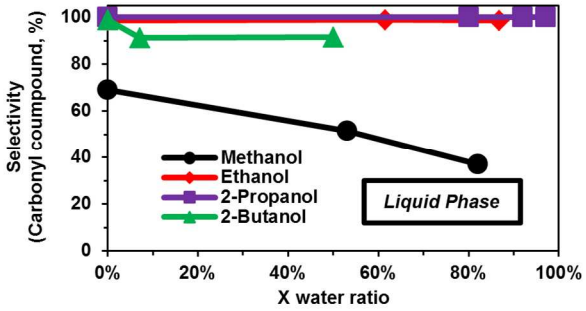

Figure 10. Water coadsorption effect on product selectivity of alcohol oxidations in the liquid phase: 7.5-15 ml pure alcohol, 0-7.5 ml distilled water, in total 15 ml volume, dissolved oxygen under 1 (C1-C3 alcohol) and 3 bar (2-butanol), 4 nm catalyst at 60 °C (C1-C3 alcohol) and 6 nm catalyst at 80 °C(2-butanol).

Figure 9 and 10 show the water coadsorption effect on the product selectivity in the gas and liquid phases. In the water-free methanol oxidation reaction in the gas phase, the selectivity was 37% of formaldehyde, and then went down gradually to 29% at the methanol to water ratio of 2:1. In C2-C4 alcohol oxidation reactions in the gas phase, the selectivity showed over 95%, remained steady regardless of the water quantity. In the liquid phase, the selectivity for

formaldehyde changed from 69 to 37% as the water ratio increase. In C2-C4 alcohol oxidation reactions in the liquid phase, the selectivity showed over 91% and insensitivity to the water quantity. These results suggest that the water coadsoption basically does not affect the product selectivity under our conditions, while it decreases the product selectivity of methanol oxidation in both gas and liquid phases. It may due to the increase of surface oxygenated species, which can further oxidize formaldehyde to formate species to methyl formate and CO_2.

3.5. Sum Frequency Generation Vibrational Spectroscopy

In order to clarify the reaction mechanism under different phase condition, we have examined SFG analysis about various alcohol species. Here 2-propanol oxidation SFG results were shown as below.[19] Figure 11 shows the correlation between reaction phase and 2-propanol molecular orientation on the catalyst surface. In the gas phase reaction condition, three vibrational peaks at ~2875 cm^{-1} (symmetric CH_3 stretch), ~2940 cm^{-1} (Fermi resonance), and ~2970 cm^{-1} (asymmetric CH_3 stretch) were detected. While in the liquid phase, the asymmetric stretch peak was increased and the symmetric stretch peak was decreased, which indicates the 2-propanol molecular orientation dependency on the reaction phase. [19,20]

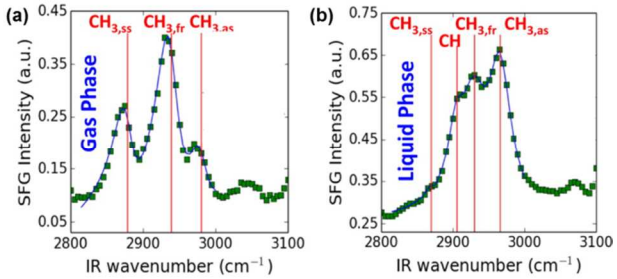

Figure 11. SFG spectra of gas (a) and liquid phase (b) 2-propanol on 4 nm Pt NPs under reaction conditions with O_2, 60°C

3.6. DFT Calculation

In order to reveal the alcohol molecular orientation possibility and how it affects to the reaction mechanism, DFT calculation was studied on 2-propanol oxidation reaction.[19] Figure 12 shows that the minimum energy configurations of 2-propanol molecules on Pt (111) surface for the gas phase (a) and liquid phase (b) conditions. In the gas phase, the 2-propanol molecules preferably orient as "lying down" on the surface while "standing up" in the liquid phase. This conformation difference can be explained by molecular steric effect; molecules have to stand up for packing in high density liquid phase. Furthermore this phenomenon induces the different distance between β-hydrogen (β-H) of the 2-propanol and Pt surface. In the previous study on alcohol oxidation reaction, the rate-limiting step is believed to be the dissociation of methylene C-H in the alkoxide assisted by oxygen.[34,35] In the table 1, the β-H-Pt distance was 4.451Å for the low concentrated condition, while 2.572Å for the high concentrated condition. It appears to be easier for the β-hydrogen to dissociate from the alkoxide species in the higher alcohol concentrated condition, which decreases the reaction activation energy in the liquid phase compared with that in the gas phase.

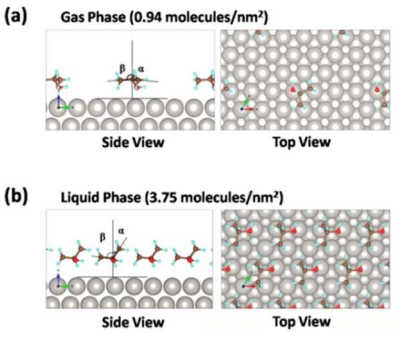

Figure 12. DFT calculation for the minimum energy configurations of 2-propanol molecules on Pt (111) surface for (a) gas phase and (b) liquid phase conditions (Pt-gray, C-brown, O-red, H-blue)

Table 1. 2-propanol molecular orientations as angles of C-C bonds relative to surface normal, adsorption energy, nearest surface-molecule distances, and nearest β-H-Pt distances for different concentrations of 2-propanol molecules on Pt (111) surface

Concentration (molecules/nm^2)	α	β	E_{ads} (eV)	$R_{surf\text{-}mol}$ (Å)	H_β-Pt (Å)
0.94	86°	86°	-0.26	3.329	4.451
3.75	38°	84°	-0.12	3.905	2.572

4. CONCLUSIONS

A wide variety of alcohol oxidations with molecular oxygen over size-controlled platinum catalyst were discussed among methanol, ethanol, 2-propanol and 2-butanol. Generally, the turnover frequency increased as the catalyst particle size became large. The activation energy in the gas phase was higher than that in the liquid phase. Water coadsorption poisoned the catalyst surface and inhibited the reaction progress in the gas and liquid phases except for the gas phase 2-butanol oxidation, while certain amount of water promoted the reaction turnover rates in the liquid phase 2-propanol oxidation. SFG and DFT analysis revealed that the alcohol molecule tends to pack horizontally on the metal surface in low concentration conditions, while it preferably stands up in high concentration conditions. The different molecular orientation of alcohol on the reaction active site affects the dissociation of the β-hydrogen of the alcohol and reaction activation energy. Further study on another alcohol oxidations catalyzed by Pt/MCF-17 is in progress and will be published soon.

ASSOCIATED CONTENT

Supporting Information

Detailed experimental procedures of Pt NPs synthesis, NPs size distribution, Pt/MCF-17 images and TOF dependence on the Pt NPs size results are included. This material is available free of charge via the Internet at http://pubs.acs.org.

AUTHOR INFORMATION

Corresponding Author

*Phone: 510-642-4053. Fax: 510-643-9668

*E-mail: somorjai@berkeley.edu

Present Addresses

§BASF Corporation, 25 Middlesex/Essex Turnpike, Iselin, NJ 08830

⊥University of Szeged, Department of Applied and Environment Chemistry, Rerrich Bela ter 1, H-6720 Szeged, Hungary

Notes

The authors declare no competing financial interest.

ACKNOWLEDGMENT

This work was supported by the U.S. Department of Energy, Office of Science, Division of Chemical Sciences, Geological and Biosciences under contract No. DE-AC02-05CH11231. H.T. acknowledges support from Nippon Shokubai Co., Ltd.

REFERENCES

(1) Feng, J.; Ma, C.; Miedziak, P. J.; Edwards, J. K.; Brett, G. L.; Li, D.; Du, Y.; Morgan, D. J.; Hutchings, G. J. Au–Pd Nanoalloys Supported on Mg–Al Mixed Metal Oxides as a Multifunctional Catalyst for Solvent-Free Oxidation of Benzyl Alcohol. *Dalt. Trans.* **2013**, *42*, 14498–14508.

(2) Davis, S. E.; Ide, M. S.; Davis, R. J. Selective Oxidation of Alcohols and Aldehydes over Supported Metal Nanoparticles. *Green Chem.* **2013**, *15*, 17–45.

(3) Vinod, C. P.; Wilson, K.; Lee, A. F. Recent Advances in the Heterogeneously Catalysed Aerobic Selective Oxidation of Alcohols. *J. Chem. Technol. Biotechnol.* **2011**, *86*, 161–171.

(4) Enache, D. I. Solvent-Free Oxidation of Primary Alcohols to Aldehydes Using Au-Pd/TiO_2 Catalysts. *Science* **2006**, *311*, 362–365.

(5) Mallat, T.; Baiker, A. Oxidation of Alcohols with Molecular Oxygen on Solid Catalysts. *Chem. Rev.* **2004**, *104*, 3037–3058.

(6) Sharma, A. S.; Kaur, H.; Shah, D. Selective Oxidation of Alcohols by Supported Gold Nanoparticles: Recent Advances. *RSC Adv.* **2016**, *6*, 28688–28727.

(7) Ciriminna, R.; Pandarus, V.; Béland, F.; Xu, Y.-J.; Pagliaro, M. Heterogeneously Catalyzed Alcohol Oxidation for the Fine Chemical Industry. *Org. Process Res. Dev.* **2015**, *19*, 1554–1558.

(8) Kopylovich, M. N.; Ribeiro, A. P. C.; Alegria, E. C. B. A.; Martins, N. M. R.; Martins, L. M. D. R. S.; Pombeiro, A. J. L. Catalytic Oxidation of Alcohols. *Adv. Organomet. Chem.* **2015**, *63*, 91–174.

(9) Slot, T. K.; Eisenberg, D.; van Noordenne, D.; Jungbacker, P.; Rothenberg, G.

Cooperative Catalysis for Selective Alcohol Oxidation with Molecular Oxygen. *Chem. - A Eur. J.* **2016**, *22*, 12307–12311.

(10) Papes Filho, A. C.; Maciel Filho, R. Hybrid Training Approach for Artificial Neural Networks Using Genetic Algorithms for Rate of Reaction Estimation: Application to Industrial Methanol Oxidation to Formaldehyde on Silver Catalyst. *Chem. Eng. J.* **2010**, *157*, 501–508.

(11) Kralj, A. K. Silver and Oxide Hybrids of Catalysts during Formaldehyde Production. *Energy* **2010**, *35*, 2528–2534.

(12) Brookes, C.; Wells, P. P.; Dimitratos, N.; Jones, W.; Gibson, E. K.; Morgan, D. J.; Cibin, G.; Nicklin, C.; Mora-Fonz, D.; Scanlon, D. O.; et al. The Nature of the Molybdenum Surface in Iron Molybdate. The Active Phase in Selective Methanol Oxidation. *J. Phys. Chem. C* **2014**, *118*, 26155–26161.

(13) Wittstock, A.; Zielasek, V.; Biener, J.; Friend, C. M.; Baumer, M. Nanoporous Gold Catalysts for Selective Gas-Phase Oxidative Coupling of Methanol at Low Temperature. *Science* **2010**, *327*, 319–322.

(14) Gandarias, I.; Nowicka, E.; May, B. J.; Alghareed, S.; Armstrong, R. D.; Miedziak, P. J.; Taylor, S. H. The Selective Oxidation of N-Butanol to Butyraldehyde by Oxygen Using Stable Pt-Based Nanoparticulate Catalysts: An Efficient Route for Upgrading Aqueous Biobutanol. *Catal. Sci. Technol.* **2016**, *6*, 4201–4209.

(15) Mistry, H.; Behafarid, F.; Zhou, E.; Ono, L. K.; Zhang, L.; Roldan Cuenya, B. Shape-Dependent Catalytic Oxidation of 2-Butanol over Pt Nanoparticles Supported on γ-Al_2O_3. *ACS Catal.* **2014**, *4*, 109–115.

(16) Ferri, D.; Baiker, A. Advances in Infrared Spectroscopy of Catalytic Solid–Liquid

Interfaces: The Case of Selective Alcohol Oxidation. *Top. Catal.* **2009**, *52*, 1323–1333.

(17) Wang, H.; An, K.; Sapi, A.; Liu, F.; Somorjai, G. A. Effects of Nanoparticle Size and Metal/Support Interactions in Pt-Catalyzed Methanol Oxidation Reactions in Gas and Liquid Phases. *Catal. Letters* **2014**, *144*, 1930–1938.

(18) Sapi, A.; Liu, F.; Cai, X.; Thompson, C. M.; Wang, H.; An, K.; Krier, J. M.; Somorjai, G. A. Comparing the Catalytic Oxidation of Ethanol at the Solid–Gas and Solid–Liquid Interfaces over Size-Controlled Pt Nanoparticles: Striking Differences in Kinetics and Mechanism. *Nano Lett.* **2014**, *14*, 6727–6730.

(19) Wang, H.; Sapi, A.; Thompson, C. M.; Liu, F.; Zherebetskyy, D.; Krier, J. M.; Carl, L. M.; Cai, X.; Wang, L.-W.; Somorjai, G. A. Dramatically Different Kinetics and Mechanism at Solid/Liquid and Solid/Gas Interfaces for Catalytic Isopropanol Oxidation over Size-Controlled Platinum Nanoparticles. *J. Am. Chem. Soc.* **2014**, *136*, 10515–10520.

(20) Thompson, C. M.; Carl, L. M.; Somorjai, G. A. Sum Frequency Generation Study of the Interfacial Layer in Liquid-Phase Heterogeneously Catalyzed Oxidation of 2-Propanol on Platinum: Effect of the Concentrations of Water and 2-Propanol at the Interface. *J. Phys. Chem. C* **2013**, *117*, 26077–26083.

(21) Wang, H.; Wang, Y.; Zhu, Z.; Sapi, A.; An, K.; Kennedy, G.; Michalak, W. D.; Somorjai, G. A. Influence of Size-Induced Oxidation State of Platinum Nanoparticles on Selectivity and Activity in Catalytic Methanol Oxidation in the Gas Phase. *Nano Lett.* **2013**, *13*, 2976–2979.

(22) Tsung, C.-K.; Kuhn, J. N.; Huang, W.; Aliaga, C.; Hung, L.-I.; Somorjai, G. A.; Yang, P. Sub-10 nm Platinum Nanocrystals with Size and Shape Control: Catalytic Study for Ethylene and Pyrrole Hydrogenation. *J. Am. Chem. Soc.* **2009**, *131*, 5816–5822.

(23) Schmidt-Winkel, P.; Lukens, W. W.; Yang, P.; Margolese, D. I.; Lettow, J. S.; Ying, J. Y.; Stucky, G. D. Microemulsion Templating of Siliceous Mesostructured Cellular Foams with Well-Defined Ultralarge Mesopores. *Chem. Mater.* **2000**, *12*, 686–696.

(24) Song, H.; Kim, F.; Connor, S.; Somorjai, G. A.; Yang, P. Pt Nanocrystals: Shape Control and Langmuir−Blodgett Monolayer Formation. *J. Phys. Chem. B* **2005**, *109*, 188–193.

(25) Zhang, Y.; Grass, M. E.; Habas, S. E.; Tao, F.; Zhang, T.; Yang, P.; Somorjai, G. A. One-Step Polyol Synthesis and Langmuir−Blodgett Monolayer Formation of Size-Tunable Monodisperse Rhodium Nanocrystals with Catalytically Active (111) Surface Structures. *J. Phys. Chem. C* **2007**, *111*, 12243–12253.

(26) Welty, J. R.; Wicks, C. E.; Wilson, R. E.; Rorrer, G. L. *Fundamentals of Momentum, Heat, and Mass Transfer 5th Edition*; John Wiley & Sons, Inc.: New York, 2007.

(27) Ferrell, R. T.; Himmelblau, D. M. Diffusion Coefficients of Nitrogen and Oxygen in Water. *J. Chem. Eng. Data* **1967**, *12*, 111–115.

(28) Stahl, B. A. S. and S. S. Mechanism of $Pd(OAc)_2$/DMSO-Catalyzed Aerobic Alcohol Oxidation: Mass-Transfer-Limitation Effects and Catalyst Decomposition Pathways. *J. Am. Chem. Soc.* **2006**, *128*, 4348–4355.

(29) Moraveji, M. K.; Sajjadi, B.; Davarnejad, R. Gas-Liquid Hydrodynamics and Mass Transfer in Aqueous Alcohol Solutions in a Split-Cylinder Airlift Reactor. *Chem. Eng. Technol.* **2011**, *34*, 465–474.

(30) Tritsaris, G. A.; Greeley, J.; Rossmeisl, J.; Nørskov, J. K. Atomic-Scale Modeling of Particle Size Effects for the Oxygen Reduction Reaction on Pt. *Catal. Letters* **2011**, *141*, 909–913.

(31) Mayrhofer, K. J. J.; Blizanac, B. B.; Arenz, M.; Stamenkovic, V. R.; Ross, P. N.;

Markovic, N. M. The Impact of Geometric and Surface Electronic Properties of Pt-Catalysts on the Particle Size Effect in Electrocatalysis. *J. Phys. Chem. B* **2005**, *109*, 14433–14440.

(32) Shao, M.; Peles, A.; Shoemaker, K. Electrocatalysis on Platinum Nanoparticles: Particle Size Effect on Oxygen Reduction Reaction Activity. *Nano Lett.* **2011**, *11*, 3714–3719.

(33) Joo, S. H.; Kwon, K.; You, D. J.; Pak, C.; Chang, H.; Kim, J. M. Preparation of High Loading Pt Nanoparticles on Ordered Mesoporous Carbon with a Controlled Pt Size and Its Effects on Oxygen Reduction and Methanol Oxidation Reactions. *Electrochim. Acta* **2009**, *54*, 5746–5753.

(34) Kobayashi, H.; Higashimoto, S. DFT Study on the Reaction Mechanisms behind the Catalytic Oxidation of Benzyl Alcohol into Benzaldehyde by O_2 over Anatase TiO_2 Surfaces with Hydroxyl Groups: Role of Visible-Light Irradiation. *Appl. Catal. B Environ.* **2015**, *170–171*, 135–143.

(35) DiCosimo, R.; Whitesides, G. M. Oxidation of 2-Propanol to Acetone by Dioxygen on a Platinized Electrode under Open-Circuit Conditions. *J. Phys. Chem.* **1989**, *93*, 768–775.

(36) Kaichev, V. V.; Popova, G. Y.; Chesalov, Y. A.; Saraev, A. A.; Zemlyanov, D. Y.; Beloshapkin, S. A.; Knop-Gericke, A.; Schlögl, R.; Andrushkevich, T. V.; Bukhtiyarov, V. I. Selective Oxidation of Methanol to Form Dimethoxymethane and Methyl Formate over a Monolayer V_2O_5/TiO_2 Catalyst. *J. Catal.* **2014**, *311*, 59–70.

(37) McCabe, R. W.; McCready, D. F. Kinetics and Reaction Pathways of Methanol Oxidation on Platinum. *J. Phys. Chem.* **1986**, *90*, 1428–1435.

(38) Alger, D. B. The Water Solubility of 2-Butanol: A Widespread Error. *J. Chem. Educ.* **1991**, *68*, 939.

TOC Graphic

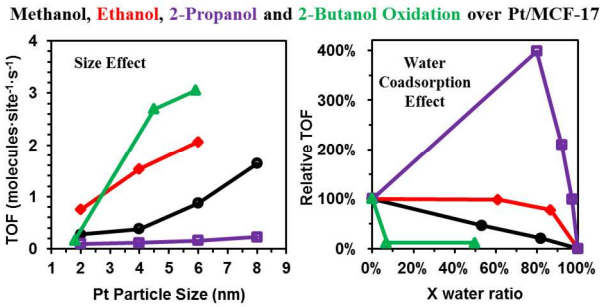
Methanol, Ethanol, 2-Propanol and 2-Butanol Oxidation over Pt/MCF-17
Size Effect
TOF (molecules·site⁻¹·s⁻¹)
Pt Particle Size (nm)
Water Coadsorption Effect
Relative TOF
X water ratio